Separation Science and Technology
Publication details, including instructions for authors and subscription information:
http://www.informaworld.com/smpp/title~content=t713708471

Ultrafilter Conditions for High-Level Waste Sludge Processing

J. G. H. Geeting[a]; R. T. Hallen[a]; R. A. Peterson[a]
[a] Pacific Northwest National Laboratory, Richland, WA, USA

To cite this Article Geeting, J. G. H. , Hallen, R. T. and Peterson, R. A.(2006) 'Ultrafilter Conditions for High-Level Waste Sludge Processing', Separation Science and Technology, 41: 11, 2313 — 2324
To link to this Article: DOI: 10.1080/01496390600742591
URL: http://dx.doi.org/10.1080/01496390600742591

Separation Science and Technology, 41: 2313–2324, 2006

ISSN 0149-6395 print/1520-5754 online
DOI: 10.1080/01496390600742591

Ultrafilter Conditions for High-Level Waste Sludge Processing

J. G. H. Geeting, R. T. Hallen, and R. A. Peterson
Pacific Northwest National Laboratory, Richland, WA, USA

Abstract: Optimal filtration conditions were evaluated for the ultrafiltration process planned for pretreating high-level waste (HLW) sludge in the Hanford Waste Treatment Plant. This sludge must be filtered in the pretreatment process to remove sodium and, consequently, reduce the number of canisters for storage. The evaluation, which was based on Hanford HLW slurry test data, was performed to identify the optimal pressure drop and crossflow velocity for filtration at both high and low solids loading. Results from this analysis indicate that the actual filtration rate achieved is relatively insensitive to these conditions under anticipated operating conditions. The maximum filter flux was obtained by adjusting the system control valve pressure to between 400 kPa and 650 kPa while the filter feed concentration increased from 5 wt% to 20 wt%. However, operating the system with a constant control-valve pressure drop of 500 kPa resulted in a reduction of less than 1% in the average filter flux. Also, allowing the control valve pressure to swing as much as $\pm 20\%$ resulted in less than a 5% decrease in filter flux. This analysis indicates that a back pressure setting of 500 kPa $\pm$ 100 kPa will give effectively optimal results for the system of interest.

Keywords: Ultrafiltration, high-level waste, concentration polarization, optimization

INTRODUCTION

Approximately 60,000 metric tons (MT) of high-level waste (HLW) sludge will be processed at Hanford's Waste Treatment Plant (WTP) to produce a final glass waste form (blended with selected soluble radioactive constituents).

Received 23 October 2005, Accepted 14 March 2006
Address correspondence to J. G. H. Geeting, Pacific Northwest National Laboratory, 902 Batelle Blvd, PO Box 989/MS P7 28, Richland, WA 99354, USA. E-mail: john.geeting@pnl.gov

However, approximately 40,000 MT of sodium commingled with the sludge must be removed to maintain a reasonable quantity of HLW glass canisters generated for storage. The methodology planned for removing the sodium involves ultrafiltration using a porous stainless steel crossflow filtration system.

The feed to the ultrafiltration process is expected to consist of approximately 5 M soluble sodium salts with 3–5 wt% insoluble solids that will be concentrated to 17–20 wt% insoluble solids. The system includes two filter trains (as depicted in Fig. 1), each with three filters in series. Each filter (of three in a series) contains two hundred and forty-one 1.27-cm-diameter tubes, 3.66 m in length. The feed to the filter is through 37 m of 30.5-cm line, while the discharge from the filter is 65 m of 30.5-cm line. Each train is fed by a single pump. The pump curve for the pump currently specified for the WTP ultrafilter is shown in Fig. 2.

The purpose of the work discussed in this paper was to identify optimal permeate flux conditions for the ultrafiltration process, in particular, to provide insight into the operating control scheme. The evaluation of filtration conditions was based on Hanford HLW slurry test data.

During the 45 years of Hanford operations, multiple processes were employed, both for plutonium processing and for special campaigns to separate other specific materials. As a result, the wastes in the underground storage tanks stem from broadly disparate origins and have significant differences in key characteristics for ultrafiltration performance. Characterization (1) of the waste has identified more than 150 different significant sludge-bearing streams. However, the HLW slurry test data used for this

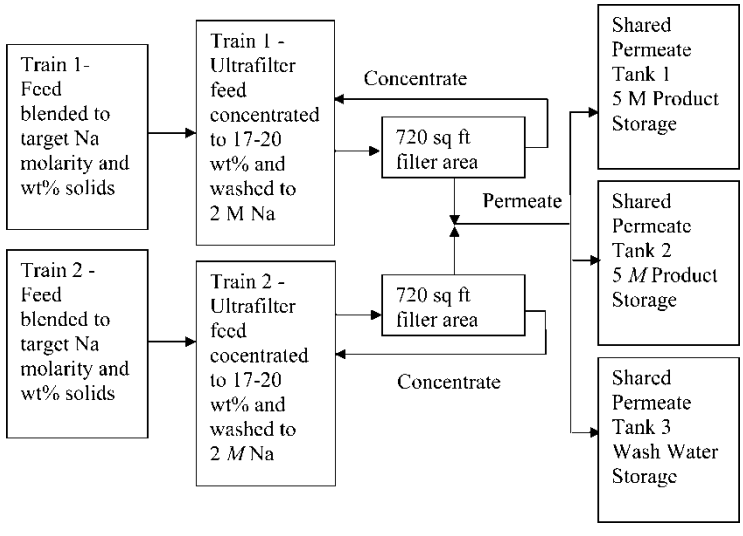

Figure 1. Schematic of WTP filtration system.

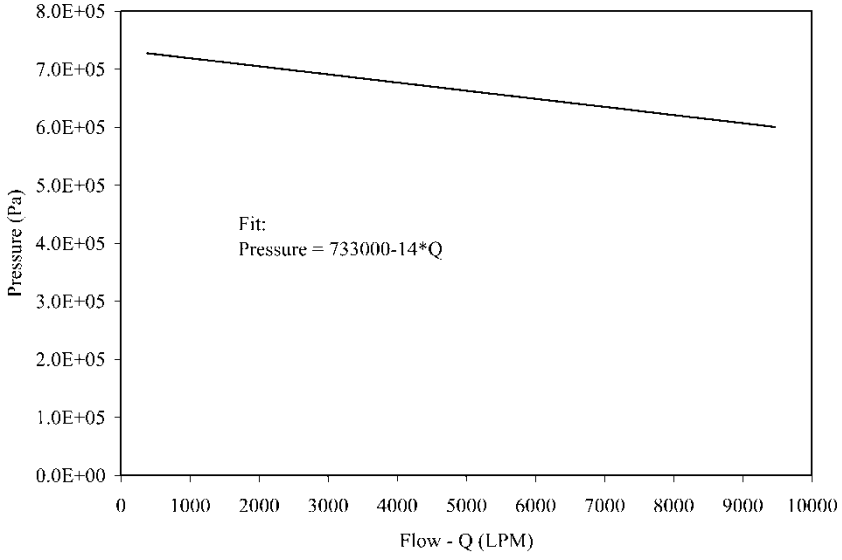

Figure 2. WTP ultrafilter pump curve.

evaluation should provide a useful picture for determining ultrafilter feed conditions.

Flux Models

A model for predicting the flux of HLW sludges, based on testing with actual waste, was developed in a previous study (2).

$$J = \frac{\Delta P}{\mu_{\text{sup}}(R_m + (\Delta P/\mu_{\text{sup}} k \ln(C_g/C)))} \tag{1}$$

where J is the permeate flux, μ_{sup} is the viscosity of the supernatant solution, R_m is the filter media resistance, and k is the mass transfer coefficient;

$$k = D_m/\delta \tag{2a}$$

where D_m is the diffusivity and δ is the boundary layer thickness. Howell et al. suggested that, for boundary layer diffusion, the diffusivity would be relatively independent of the slurry viscosity (3). However, the boundary layer thickness should be dependent on the viscosity and velocity of the solution (4).

$$k = \frac{D_m}{\delta} \propto D_m \alpha \sqrt{\frac{V}{\mu_{\text{slurry}}}} = k' \sqrt{\frac{V}{\mu_{\text{slurry}}}} \tag{2b}$$

Substituting equation (2b) into equation (1) yields:

$$J = \frac{\Delta P}{\mu_{\text{sup}}(R_m + (\Delta P/k'\mu_{\text{sup}}\sqrt{(V/\mu_{\text{slurry}})}\ln(C_g/C))} \tag{3}$$

It is also necessary to understand the frictional losses associated with flow through pipes. This classically is defined for turbulent flow by:

$$f = \frac{0.0791}{\text{Re}^{1/4}} \tag{4}$$

where

$$f = \frac{D}{L}\frac{\Delta P}{2\rho V^2} \tag{5}$$

$$\text{Re} = \frac{DV\rho}{\mu_{\text{slurry}}} \tag{6}$$

Data used in this analysis were primarily derived from Hanford Tank AZ-101 (5). Rheological testing of the slurry samples from this tank indicates that the slurry acts as a Bingham plastic with a yield stress generally <3 Pa. Beyond this yield stress, typical Newtonian liquid behavior prevails. Although pressure-drop calculations using Newtonian turbulent flow equations are not rigorously correct, such treatment is believed to be satisfactory for this analysis.

EXPERIMENTAL

This evaluation was based on earlier experiments (5) using a new, 0.1-μm Mott filter tube with a 61-cm active length, 1-cm-ID bore and 0.16-cm wall thickness. An Oberdorfer progressive capacity pump (powered by an air motor) propels the slurry from a reservoir through the magnetic flow meter (Fischer & Porter) and the filter element. The axial velocity and ΔP are controlled by the pump speed and the throttle valve position. Permeate that passes through the filter can be removed or reconstituted with the slurry in the reservoir. The permeate flow rate is measured by a graduated glass-flow monitor or, for higher flow rates, an in-line rotameter.

During the tests, the slurry temperature was maintained at 25 ± 5°C by pumping cooling water through a shell-and-tube heat exchanger just downstream of the magnetic flow meter. The supernatant had a viscosity of approximately 4.1×10^{-3} Pa-s at 25°C. In previous testing, the slurry viscosity was found to change as a function of the solids content. Figure 3 summarizes the viscosity data for a variety of HLW slurries. Note that these data were obtained from a number of HLW samples (5–7) and, as such, significant sample variability has been introduced. However, the trend of increasing

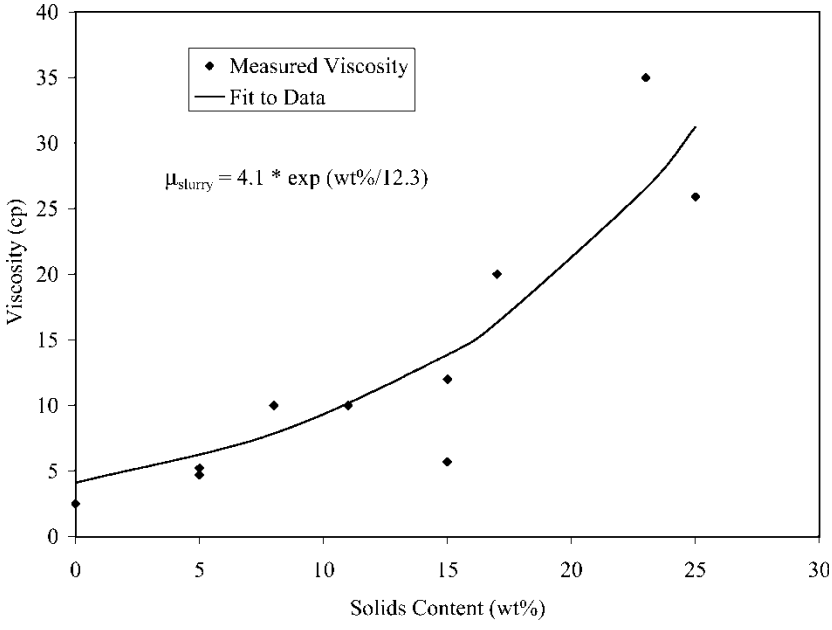

Figure 3. Effect of insoluble solids content on slurry viscosities.

viscosity with increasing solids content is as expected. Further, the rapid increase in viscosity at higher solids content, >20 wt%, is consistent with all experimental evidence for these materials. Figure 3 also provides a fit to the experimental data based on the assumption that the viscosity at 0 wt% must be the same as the supernatant viscosity. Densities of the solution were approximately 1200 kg/m.[3]

A test matrix consisting of 13 combinations of transmembrane pressures and crossflow velocities was completed. The first condition (center point) was held for 3 hours before conditions were changed with a backpulse each hour. The center point was then repeated in the middle and at the end of testing to assess the effect of filter fouling over the course of testing. This test matrix was completed for two different feed conditions, 7.6 wt % and 17.9 wt%.

RESULTS

Figure 4 provides the flux data from the filtration test with AZ-101 and presents a plot of the least squares fit to these data using equation (3) with the slurry rheology fit shown in Fig. 3. As noted above, differing feed conditions were tested at 7.6 wt% and 17.9 wt%. Figure 5 illustrates the least squares fit to the data at constant velocity over a range of pressures at these

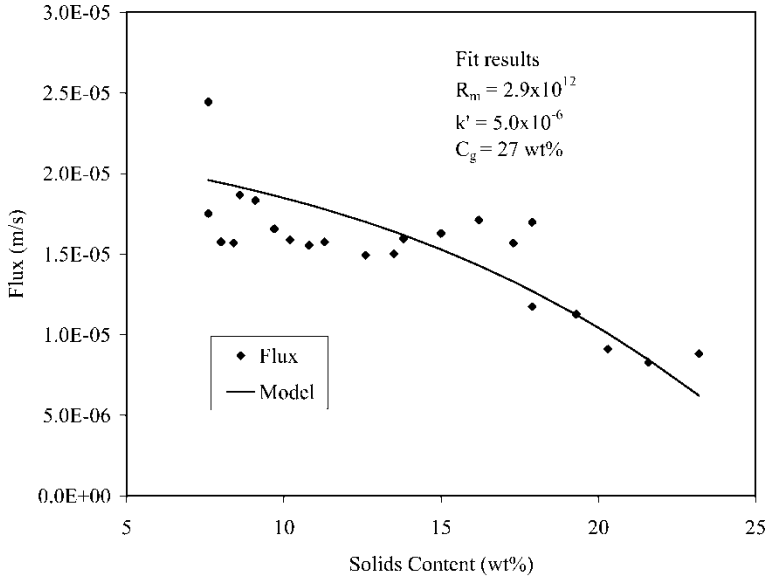

Figure 4. Effect of slurry insoluble solids content on filter flux.

two conditions. Figures 4 and 5 indicate that the model provides a reasonable fit to the experimental data. It can be seen that the model overpredicts the flux at high pressure, likely because the model underpredicts the resistance from the filter cake layer under both conditions. This fit to the data could be improved by additional testing at lower solids concentrations and by additional rheology data under better controlled conditions. Taken as a whole, equation (3) provides a reasonable prediction of performance and can be used to provide insight into the planned operating conditions for the full-scale process filters.

Because the total length of the filter media is $\sim$11 m, there will be a significant pressure drop across it. Using the empirical models established in Figs. 3 and 4 and the planned configuration of the WTP filter system, it is possible to estimate the pressure profile for the filter elements. It is anticipated that the performance of the filter during WTP operation will be controlled by the back pressure on the outlet from the third filter element. As such, this is the starting point for calculating pressure drop. The velocity down the tubes is:

$$V = \frac{Q}{1000 \cdot 60 \cdot A} = \frac{4Q}{241 \cdot 60000\pi D^2} = 0.00055Q \qquad (7)$$

where V is the velocity down a tube in m/s, A is the cross-sectional area of the tube sheet in m,^{2} D is the diameter of the individual tubes in m, and Q is the flux in L/min. Then, assuming that the filter and control valve

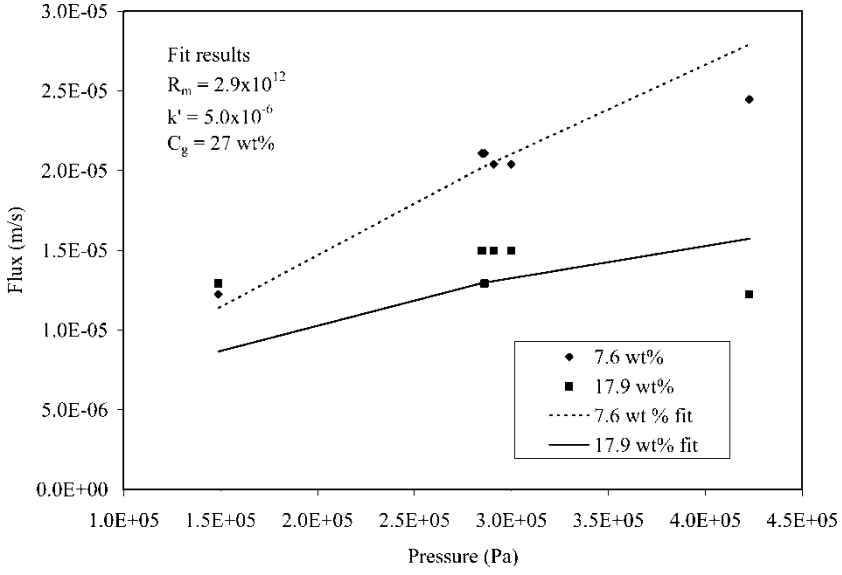

Figure 5. Effect of transmembrane pressure on filter flux.

dominate the line losses in the system, the filter outlet pressure from the pump can be calculated for a back pressure setting:

$$P_{\text{dis}} = \Delta P + P_{cv} = V^2 \frac{L}{R} f\rho + P_{cv} = V^2 \frac{L}{R} \rho \frac{0 \cdot 0791}{\text{Re}^{1/4}} + P_{cv} \qquad (8)$$

The pump discharge pressure from the pump curve in Fig. 2 follows:

$$P_{\text{dis}} = 733000 - 14Q \qquad (9)$$

Substituting equation (7) into equation (8) and equating to equation (9) gives

$$P_{\text{dis}} = 3.0 \times 10^{-7} Q^2 \frac{L}{R} \rho \frac{0.0791}{(\cdot 00055 QD\rho/\mu_{\text{slurry}})^{1/4}} + P_{cv}$$

$$= 733000 - 14Q \qquad (10)$$

Equation (10) will yield one unique real solution for Q for any given set of physical parameters. Figure 6 shows these solutions for selected solids contents in the waste, and indicates the resultant axial velocity in the system as a function of the control valve setting. For each point on Fig. 6, there would be a corresponding flux profile across the filter. Figure 7, which provides the profiles for differing valve settings for 5 wt% insoluble solids, shows that the flux will vary along the length of the filter tube as a result of the pressure drop along the filter. Figure 7 also suggests that the optimal

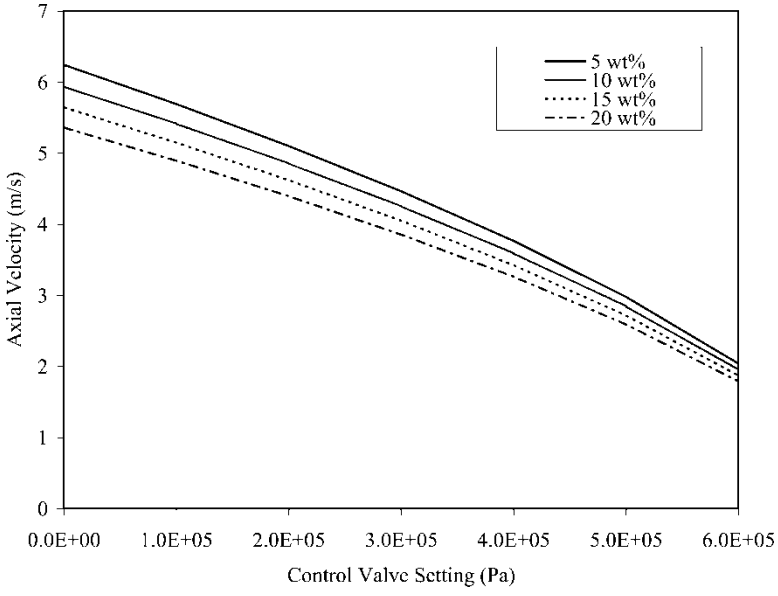

Figure 6. Effect of control valve setting on axial velocity.

flux for 5 wt% material (integrated over the length of the filter) is achieved at higher control valve settings. However, a more accurate assessment of the performance can be obtained by determining the average flux for the whole filter element.

Equation (5) can be re-written as:

$$\Delta P = \frac{Lf}{R}\rho V^2 \tag{11}$$

Substituting equation (11) into equation (3) yields

$$J = \frac{P_{CV} + (Lf/R)\rho V^2}{\mu_{\text{sup}}(R_m + (P_{CV} + (Lf/R)\rho V^2)/(k'\mu_{\text{sup}}\sqrt{(V/\mu_{\text{slurry}})}\ln(C_g/C)))} \tag{12}$$

It is useful to make some substitutions:

$$a = \frac{f\rho V^2}{R} \tag{13}$$

$$b = k'\sqrt{\frac{V}{\mu_{\text{slurry}}}}\ln(C_g/C) \tag{14}$$

$$c = \mu_{\text{sup}}R_m \tag{15}$$

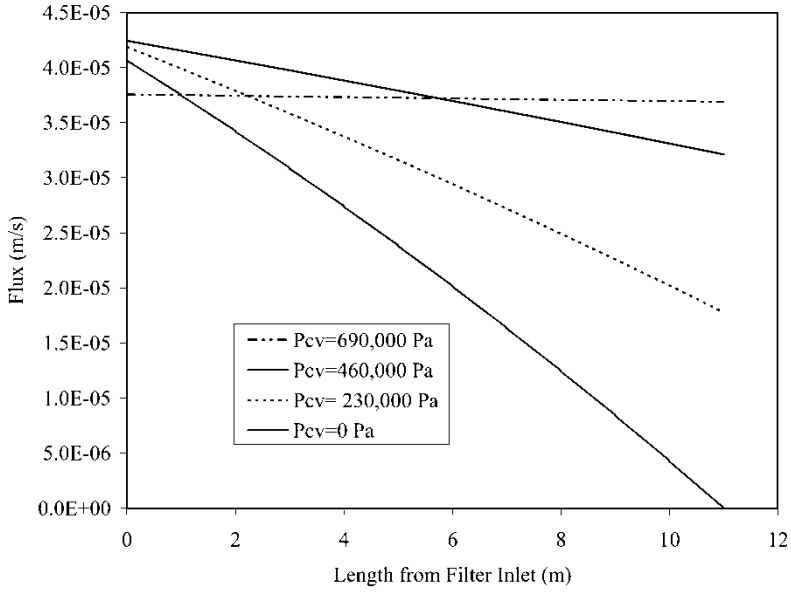

Figure 7. Filter flux along porous filter tube length.

Integration of equation (12) gives

$$\int \frac{a \cdot L + P_{CV}}{c + (a \cdot L + P_{CV}/b)} dL = b\left(L - \frac{b \cdot c \cdot \ln[b \cdot c + a \cdot L + P_{CV}]}{a}\right)\Bigg|_0^L \quad (16)$$

It should be noted that the slurry density and apparent viscosity will change slightly over the length of the filter as the permeate is removed. These small changes are not accounted in this integration. Thus, the average flux for the filter is

$$\bar{J} = b + \frac{c \cdot b^2}{L \cdot a}(\ln[b \cdot c + P_{CV}] - \ln[b \cdot c + a \cdot L + P_{CV}]) \quad (17)$$

Figure 8 plots the average flux for various control valve settings for a number of selected solids contents and indicates, as expected, that the higher the solids content, the lower the dependency of filter flux on back pressure. Physically, this result is associated with the fact that the filtrate flux may be limited either by the viscous resistance of the fluid passing through the porous media (filter media and filter cake) or by the capability of the fluid to transport accumulated solids away from the filter cake.

At higher solids content, the filtrate flux loses pressure dependency, as an increase in pressure results in a corresponding increase in the filter cake (or gel layer) and little to no increase in the steady-state filtrate flux. This is illustrated in Fig. 9 by plotting the average filter flux during concentration from 5 wt% to

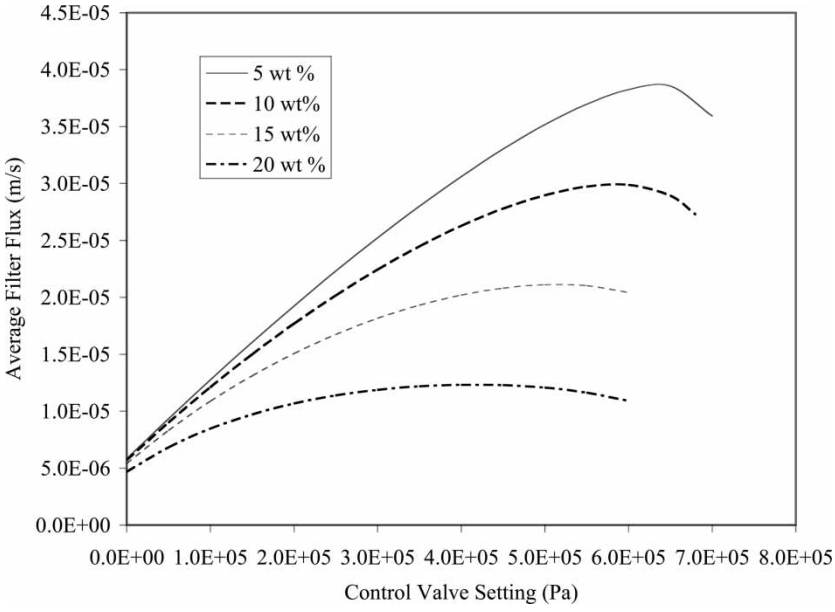

Figure 8. Average filter flux at various solids loadings.

20 wt% at a given back pressure. The average flux calculated and the shape of the curve shown in Fig. 9 appears to most closely resemble the curve for 15 wt% in Fig. 8. This is because as the solids loading increases from 5 to 20 wt%, the flux declines and consequently the average flux during the concentration is more heavily weighted by the flux at higher solids loadings. As can be seen in Fig. 9, the concentration process is very insensitive to the back pressure setting. The optimum is achieved at a back pressure setting of approximately 500 kPa. However changing the setting by up to 100 kPa results in a less than 5% decrease in average filter flux.

CONCLUSIONS

An analysis was performed on available experimental filtration data for Hanford HLW slurries. During previous ultrafiltration testing, a significant portion of the effort focused on identifying the optimal filtration conditions, with an emphasis on identifying a target pressure at which to operate. However, results from this analysis suggest that, in practical application, the performance of the filtration system will be relatively insensitive to the back pressure selected (in the range of 300 to 600 kPa). Consequently, this analysis suggests that a back pressure setting of 500 kPa $\pm$ 100 kPa will give effectively optimal results for the system of interest.

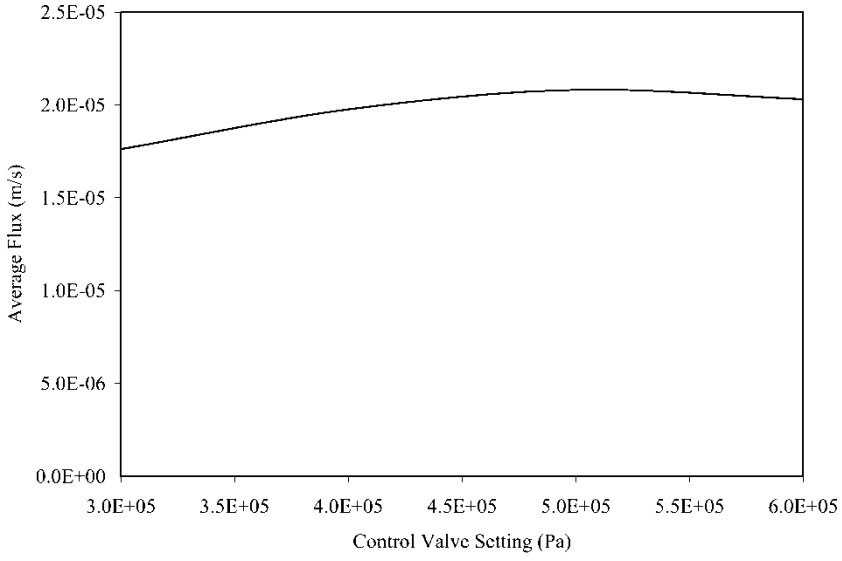

Figure 9. Average filter flux during concentration of slurry from 5 wt% to 20 wt% insoluble solids.

The evaluation discussed here was based primarily on slurry samples from a single tank. It is anticipated that other tanks would be characterized by slightly different filtration parameters. This analysis would further benefit from additional data associated with the viscosity of HLW slurries and the filtration performance of these slurries over a broader range of feed conditions and, in particular, test data at lower solids concentrations. However, the general conclusions regarding the variability of performance as a function of the primary control parameter (i.e., control valve setting) are likely applicable across a wide range of feed materials.

NOMENCLATURE

A	area (m^2)
C_g	gel concentration (wt% insoluble solids); i.e., the solids concentration at the filter membrane, which according to the gel polarization model, is assumed to have a fixed solids concentration, but is free to vary in thickness or porosity.
C	feed concentration (wt% insoluble solids)
D	diameter (m)
D_m	diffusion coefficient (m^2/s)
J	flux through the filter (m/s)
k	mass transfer coefficient (m/s)

k'	modified mass transfer coefficient ($kg^{0.5}/s$)
L	pipe length (m)
ΔP	differential pressure, along pipe length or across filter membrane (Pa)
P_{dis}	pump discharge pressure (Pa)
P_{cv}	pressure immediately upstream of the control valve (Pa)
Q	volumetric flow rate (liter/min)
R	radius (m)
R_m	membrane resistance (m^{-1})
R_g	gel layer resistance (m^{-1})
V	velocity (m/s)
α	unit conversion parameter ($kg^{0.5}/m^2$)
δ	boundary layer thickness (m)
ρ	density (kg/m^3)
μ	viscosity (Pa-s)

REFERENCES

1. Tran, T.T., Bobrowski, S.F., Lang, L.L., and Olund, T.S. (2000) *Best-Basis Inventory Maintenance Tool (BBIM): Database Description and User Guide*; CH2M Hill Hanford Group: Richland, WA.
2. Geeting, J.G.H., Hallen, R.T., and Peterson, R.A. (2005) Optimization of ultrafilter feed conditions using classical filtration models. *Journal of Membrane Science*, 265: 137–141.
3. Howell, J., Field, R., and Dengxi, W. (1996) Ultrafiltration of high-viscosity solutions: theoretical developments and experimental findings. *Chem. Eng. Sci.*, 51 (9): 1405–1415.
4. Bird, R.B., Stewart, W.E., and Lightfoot, E.N. (1960) *Transport Phenomena*; Wiley: New York.
5. Geeting, J.G.H., Hallen, R.T., Jagoda, L.K., Poloski, A.P., Scheele, R.D., and Weier, D.R. (2003) *Filtration, Washing, and Caustic Leaching of Hanford Tank AZ-101 Sludge*; Pacific Northwest Division: Richland, WA, PNWD-3206, Rev. 1, Battelle.
6. Brooks, K.P., Bredt, P.R., Golcar, G.R., Hartley, S.A., Jagoda, L.K., Rappe, K.G., and Urie, M.W. (2000) *Characterization, Washing, Leaching, and Filtration of C-104 Sludge*; British Nuclear Fuels, Limited: Richland, WA, PNWD-3024, Battelle, Pacific Northwest Division, and BNFL-RPT-030, Rev. 0.
7. Brooks, K.P., Bredt, P.R., Cooley, S.C., Golcar, G.R., Jagoda, L.K., Rappe, K.G., and Urie, M.W. (2000) *Characterization, Washing, Leaching, and Filtration of AZ-102 Sludge*; British Nuclear Fuels, Limited: Richland, WA, PNWD-3045, Battelle, Pacific Northwest Division, and BNFL-RPT-038, Rev. 0.